Moisture Resistance of Insulating Films for Compound Semiconductor Devices

Tomoki Oku[1], Manabu Okumura[2], Masahiro Totsuka[1], Toshihiko Shiga[1] and Masayoshi Takemi[1]

[1] Mitsubishi Electric Corporation, High Frequency & Optical Device Works
[2] Melco Semiconductor Engineering Corporation
[1, 2] 4-1 Mizuhara, Itami, Hyogo 664-8641, Japan
Phone: +81-72-784-7239, Fax: +81-72-780-2683, E-mail: Oku.Tomoki@ap.MitsubishiElectric.co.jp

Key words: Moisture resistance, silicon nitride, silicon oxide, pressure cooker test, FTIR.

Abstract

We demonstrate that differences in moisture resistance can be explained by film oxidation and changes in defect densities evaluated by Fourier-transform infrared spectroscopy. The insulating film with the highest moisture resistance was a stoichiometric silicon nitride (Si_3N_4) film with a refractive index of 2.1 and containing the least N–H bonds. We propose that the density of N–H bonds is a more appropriate index of moisture resistance than the refractive index by considering the oxidation mechanism of silicon nitride (SiN_x), silicon oxynitride (SiO_xN_y), and silicon oxide (SiO_x) films.

INTRODUCTION

Si_3N_4 films are widely used to protect the surface of semiconductor devices because they are more resistant to humidity than silicon dioxide (SiO_2). However, depositing silicon nitride (SiN_x) films at low temperatures with plasma-enhanced chemical vapor deposition (PE-CVD)—a common process in compound semiconductor devices—generates a high density of Si–H and N–H bonds, which may explain the poorer moisture resistance of SiN_x films versus Si_3N_4 films deposited at high temperatures. Moreover, operating compound semiconductor devices at microwave frequencies requires the device to have low parasitic capacitance. Because of these requirements, many wish to develop a fabrication method that decreases the film thickness and dielectric constant of silicon nitride films while maintaining moisture resistance. We have worked to manufacture microwave devices with various insulating films [1]. Along with this, we have studied a technique to evaluate moisture resistance by comparing Fourier-transform infrared (FTIR) absorption spectra before and after a pressure cooker test (PCT) [2]. In the present paper, we demonstrate that moisture resistance can be compared by evaluating film oxidation and the changes in defect density from FTIR spectra.

EXPERIMENTS

The Si_3N_4, SiN_x, SiO_xN_y and SiO_x films were deposited on GaAs wafers at ~300 °C by catalytic chemical vapor deposition (Cat-CVD) and by various types of PE-CVD, as shown in Table I. The film thickness was ~50 nm on both sides of the wafers. The moisture resistance of the insulator films was examined by a PCT in water vapor at 2 atm and 121 °C for 96 h. The oxidation ratio of the films was estimated by evaluating the Si–O and Si–N peak areas from FTIR spectra (MFT-2000; JASCO Corporation). The densities of Si–H, O–H, and N–H bonds in the insulator films were also estimated from FTIR absorption spectra [2]. To convert the absorption bands to bond densities, we used the absorption cross-sections of the Si–H and N–H bonds in the SiN_x film [3] and the Si–H and O–H bonds in the SiO_x film [4]. We did not consider the oxidation of the GaAs substrates because the FTIR signals for the Ga–O and As–O bonds (~500 cm^{-1}) are outside of the measurement range of the instrument. We denote the densities of X–Y bonds by using [X–Y] in this paper. To analyze the wavenumber from the FTIR absorption spectra and assess the diffusion barrier for H_2O and NH_3 molecules in the insulator films, we used semi-empirical molecular orbital calculations [5]. The model clusters comprised several hundred atoms based on their crystal structures: high-cristobalite SiO_2, Si_2N_2O, and beta-Si_3N_4 belong to the space groups O_h^7(Fd3m), C_{2v}^{12}(Cmc2$_1$), and C_{6h}^2(P6$_3$/m), respectively [6]. When we assessed SiO_x clusters with an O–H bond, we removed a silicon atom and terminated the oxygen dangling bonds with hydrogen atoms.

TABLE I
Insulator films fabricated for humidity tests.

Film	Deposition	Refractive Index	Permittivity
Si_3N_4	Cat-CVD	2.1	7
SiNx	PE-CVD	1.7 – 2.0	6 - 7
SiOxNy	PE-CVD	1.7	5
SiOx	PE-CVD	1.5	4

RESULTS AND DISCUSSION

Figure 1 shows examples of FTIR absorption spectra for insulating films prepared by Cat-CVD and PE-CVD before and after the PCT. For the Cat-CVD Si_3N_4 films (Fig. 1(a)), the PCT led to few changes in the Si–O and Si–N bond peaks. For the PE-CVD SiN_x films (Fig. 1(b)), the PCT caused a Si–O bond peak to appear ~1100 cm^{-1} and

9

decreased the intensity of the Si–N bond peak at ~800 cm^{-1}. These changes were caused by oxidation from moisture penetrating into the SiN_x films. For the PE-CVD SiO_xN_y and SiO_x films (Fig. 1(c) and (d)), the PCT sharpened the Si–O bond peak at ~1076 cm^{-1} and extinguished the Si–N bond peak at ~800 cm^{-1}.

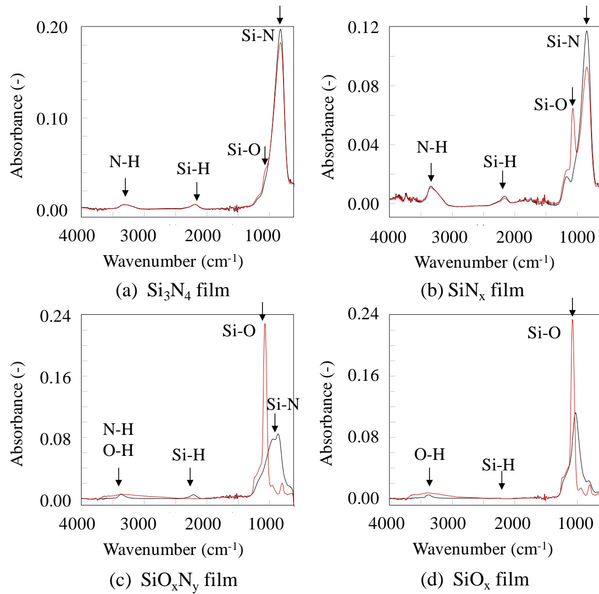

Figure 1. FTIR absorption spectra (black spectra) before and (red spectra) after the PCT. Sample (a) was prepared by Cat-CVD, while samples (b–d) were prepared by PE-CVD.

Figure 2 shows extended FTIR absorption spectra from 1500 to 4000 cm^{-1}. For the Si_3N_4 and SiN_x films (Figs. 2(a) and (b)), the PCT caused few changes in the FTIR signal for the N–H and Si–H bond peaks at ~2200 cm^{-1} and ~3350 cm^{-1}, respectively. The PCT broadened the O–H or N–H bond peaks in the SiO_xN_y films (Fig. 2(c)) and the O–H bond peak in the SiO_x films (Fig. 2(d)). We believe the broad absorption peaks from 2200 to 3750 cm^{-1} to be composed of three different components because they have outstanding inflection points at ~3000 cm^{-1} and ~3500 cm^{-1}. The PCT suppressed the Si–H bond peak in the SiO_xN_y films. In contrast, the FTIR signal from the Si–H bond peak in the SiO_x films was too small both before and after PCT to note any change. To analyze this small signal we considered the peak area, which we calculated by integrating the absorption in the spectra; we will discuss this calculation later in the paper.

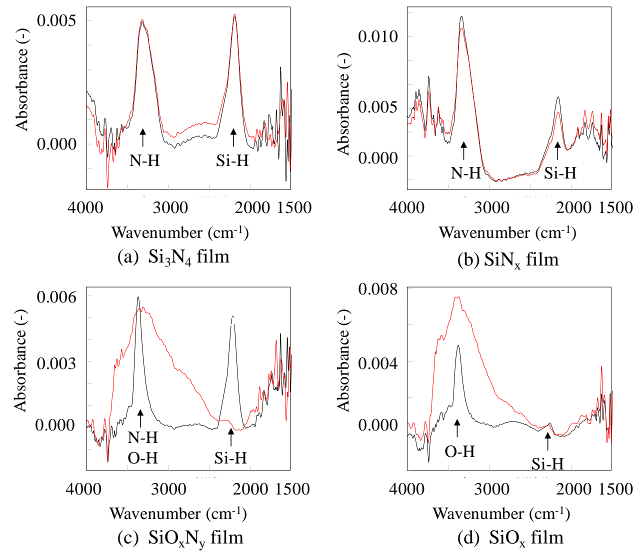

Figure 2. Extended FTIR absorption spectra (1500–4000 cm^{-1}) for the insulating films (black spectra) before and (red spectra) after PCT.

Figure 3 shows the Si–O and Si–N composition ratios before and after PCT, which we calculated from the peak area of the FTIR signal. The Si–O and Si–N composition ratios are defined by [Si–O] / ([Si–N] + [Si–O]) and [Si–N] / ([Si–N] + [Si–O]), respectively. The PCT did not drastically change the Si–O and Si–N composition ratios for the SiN_x and Si_3N_4 films. In contrast, the PCT changed those ratios drastically in the SiO_xN_y and SiO_x films. Because the changes in these ratios are indices of oxidation and de-nitrification, these results show that the properly deposited SiN_x and Si_3N_4 films were much more resistant to humidity than the SiO_xN_y and SiO_x films. The Si_3N_4 film was most resistant to oxidization and thus to moisture.

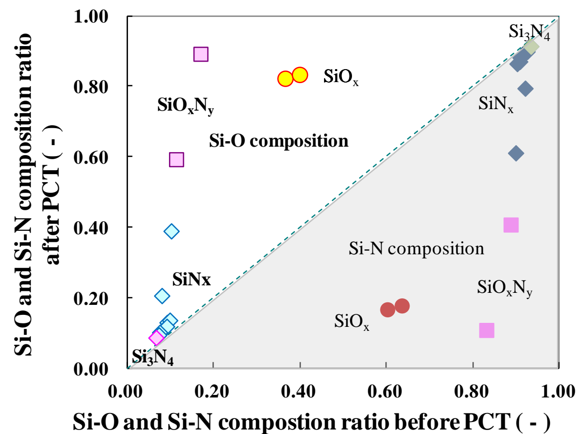

Figure 3. Composition ratios of Si–O and Si–N, before and after the PCT.

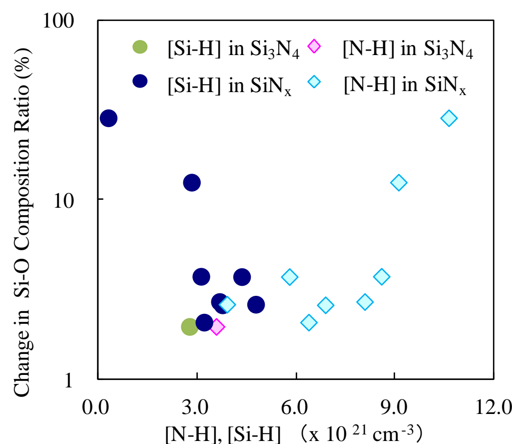

Figure 4. Oxidation of the silicon nitride films by the PCT.

To analyze the moisture resistance of the SiN_x and Si_3N_4 films, we show in Fig. 4 how the Si–O composition ratio changed after the PCT based on [Si–H] and [N–H]. We obtained the change in Si–O composition ratio by comparing [Si–O] / ([Si–N] + [Si–O]) before and after the PCT. Less oxidation occurred at lower [N–H], but oxidation did not depend on [Si–H].

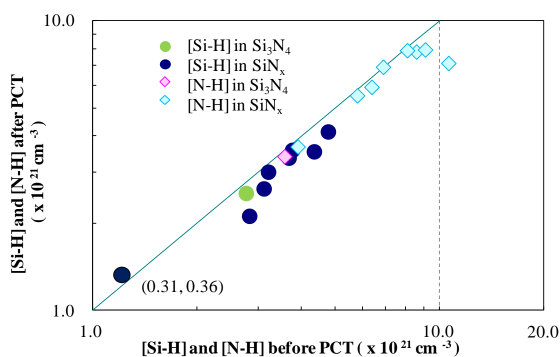

Figure 5. Densities of Si–H and N–H bonds in the SiN_x and Si_3N_4 films before and after the PCT.

To show how the Si–H and N–H bonds influenced oxidation, in Fig. 5 we show how the PCT changed the densities of [Si–H] and [N–H] in the SiN_x and Si_3N_4 films. Both [Si–H] and [N–H] remained unchanged after PCT. Wet oxidation does not create additional O–H and Si–H bonds based on the following reaction: $Si_3N_4 + 6\ H_2O \rightarrow 3\ SiO_2 + 4\ NH_3$. Breakage of Si–N bonds by H_2O molecules involves hydroxide ions attacking Si atoms and hydrogen ions attacking N atoms, as in HF etching [7]; the oxidation reaction sequence in silicon nitride can be expressed as:

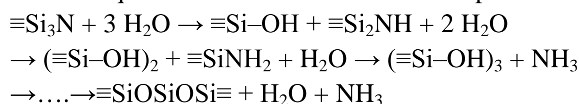

$\equiv Si_3N + 3\ H_2O \rightarrow \equiv Si\text{–}OH + \equiv Si_2NH + 2\ H_2O$

$\rightarrow (\equiv Si\text{–}OH)_2 + \equiv SiNH_2 + H_2O \rightarrow (\equiv Si\text{–}OH)_3 + NH_3$

$\rightarrow \ldots . \rightarrow \equiv SiOSiOSi\equiv + H_2O + NH_3$

Here, ≡Si–X denotes a Si atom terminated by X and ≡Si denotes a Si atom and three back bonds connected to either N or O atoms. This reaction explains why the Si_3N_4 film with the least [N–H] was most resistant to moisture: the N–H bonds help create NH_3 molecules by skipping the first step of the reaction chain. However, the SiO_x film created by the PCT is of low quality because the PCT temperature was lower than the standard temperature for oxidizing silicon, ~1000 °C [8].

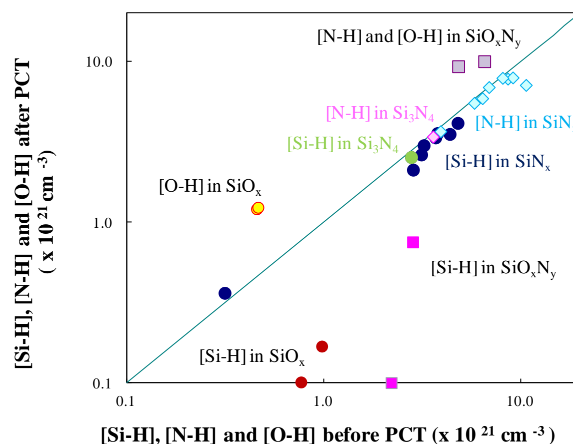

Figure 6. Densities of Si–H, N–H, and O–H bonds in the SiO_xN_y and SiO_x films before and after the PCT, plotted to contrast those of the SiN_x and Si_3N_4 films.

To investigate the characteristics of the poor-quality SiO_x film, in Fig. 6 we show the [Si–H], [O–H], and [N–H] densities in the SiO_xN_y and SiO_x films before and after the PCT. For the SiO_xN_y and SiO_x films, the increases in [N–H] and [O–H] after the PCT contrast the large decrease in [Si–H]. If the SiO_xN_y film is composed of Si_2N_2O and defects, a wet oxidation reaction does not create additional O–H and Si–H bonds based on the following reaction: $Si_2N_2O + 3\ H_2O \rightarrow 2\ SiO_2 + 2\ NH_3$. Thus, we assume the SiO_xN_y film to be composed of Si_3N_4, Si_2N_2O, and SiO_2, which explains the creation of bonds in the SiO_xN_y and SiO_x films. Also, the density of N–H bonds should not increase in the presence of excess H_2O molecules. Based on these assumptions and reasonings, we will now discuss the creation of O–H bonds in the SiO_x film.

First, we believe the increase in [O–H] to be related to creation of O–H bonds from the following reaction between excess H_2O molecules and the SiO_2 network: H_2O + ≡Si–O–Si≡ → ≡Si–OH + HO–Si≡. While the broad peak from 2200 to 3750 cm^{-1} cannot be explained by increases in ≡Si–OH (O–H bonds), we attribute the broad peak from 3000 to 3750 cm^{-1} to the following structures: 1) molecular water that is free, hydrogen-bonded, or structurally bound; 2) O–H bonds, hydrogen-bonded to neighboring O–H bond groups; 3) H_2O molecules; 4) O–H bonds (3672 cm^{-1}) [9]. A molecular orbital calculation (Fig. 7) shows that, to explain the broad absorption from 2200 to 3000 cm^{-1}, we must assume a structure with excess oxygen,

such as a hydrogen-terminated peroxy radical (SiO–OH). However, we cannot propose the SiO–OH formation process at the present time because it does not seem to be related to water oxidation, as shown by this reaction: ≡Si–OH + H_2O → ≡SiO–OH + H_2.

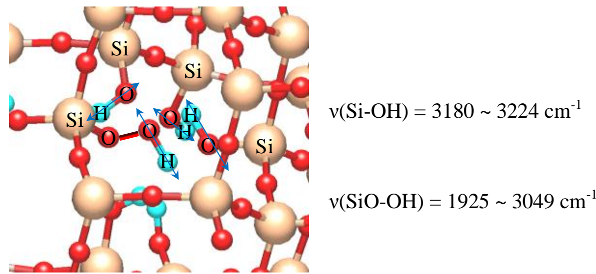

Figure 7. Modeled cluster of SiO─OH and Si─OH bonds in a SiO_x film and the respective wavenumbers (ν), derived from a molecular orbital calculation.

Second, we believe the decrease in [Si–H] is related to the following reaction: ≡Si–H + $3H_2O$ → $SiH(OH)_3$ (aq) + 3/2 H_2. This reaction etches the SiO_x film because $SiH(OH)_3$ is likely soluble in water, forming a compound such as $Si(OH)_4$ [10]. Unfortunately, our FTIR spectra could not show that etching occurred because it was not sufficiently sensitive to detect small changes in atomic compositions in the film.

Finally, to discuss the penetration of H_2O molecules into the films, we derived energy barriers from molecular orbital calculations. The penetration barriers for the Si_3N_4, SiN_x, Si_2N_2O, and SiO_2 films are 2.1, 1.8, 1.6, and 0.5 eV, respectively [11]. Because the penetration barrier is the activation energy of interstitial diffusion, the unknown actual diffusion barriers are considered to be in the corresponding barrier of interstitial diffusion. If we consider the oxidized Si_3N_4 and SiN_x films to be Si_2N_2O and SiO_2 films, this oxidation lowers the diffusion barrier, easing the diffusion of H_2O and NH_3 molecules into the oxide films versus the Si_3N_4 and SiN_x films, although we have not yet investigated the diffusion of NH_3 molecules.

Figure 8 summarizes the oxidation process in the presence of moisture: the H_2O molecules attack the surface of the silicon nitride; the H_2O molecules diffuse into the silicon nitride; the bulk silicon nitride oxidizes from breakage of Si–N bonds and generation of Si–O and N–H bonds; NH_3 molecules form and diffuse out of the silicon oxide (oxynitride) to desorb from the surface of the silicon oxide. Considering the oxidation mechanism of silicon [8], the oxide thickness x_o after a long time can be expressed as $x_o^2 = Bt$, where t is the oxidation time and B is a parameter proportional to the diffusivity of the H_2O molecules in the oxide layer. Silicon oxidation is universally controlled by the thermal silicon dioxide and the silicon substrate. The oxidation of the insulator film depends on the film species, the film quality, the humidity, the pressure, and the temperature. Therefore, the [N–H] in the silicon nitride and the [O–H] in the oxide layer can be sensitive indices for moisture resistance, which is inversely proportional to the growth rate of the oxide and the quality of the oxide layer.

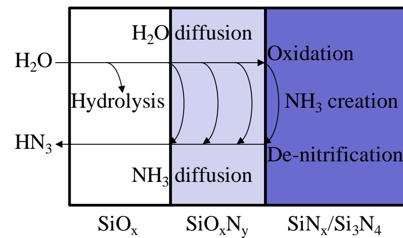

Figure 8. Schematic of oxidation in a silicon nitride film.

Conclusions

The most moisture-resistant film was the stoichiometric silicon nitride (Si_3N_4) film with a refractive index of 2.1 and minimum [N–H]. We propose that [N–H] is a more appropriate index for moisture resistance than the refractive index, because the N–H bonds help create NH_3 molecules during oxidation of silicon nitride. We demonstrated that the moisture resistance of the SiO_xN_y and SiO_x films rapidly decreased after PCT because their surfaces easily changed to low-quality oxide films containing excess H_2O molecules and many O–H bonds.

Acknowledgement

We express our sincere thanks for the technical assistance given by our colleagues at the Mitsubishi Electric Corporation.

Acronym

Cat-CVD: Catalytic Chemical Vapor Deposition

References

[1] T. Oku, Y. Kamo and M. Totsuka, Thin Solid Films 516 (2008) 545.
[2] A. Masuda, M. Totsuka, T. Oku, R. Hattori and H. Matsumura, Vacuum vol.74, (2004), 525.
[3] W. A. Lanford and M. J. Rand, J. Appl. Phys. 49 (1978)2473
[4] K. H. Beckmann et al., J. Electrochem. Soc. 118 (1971) 614
[5] MO-G Version *1.0.6*, Fujitsu Limited, Tokyo, Japan (*1997-2011*).
[6] Ralph W. G. Wyckoff, Crystal Structures, 2nd ed., John Wiley & Sons, New York (1964).
[7] T. Oku, K. Sato and M. Otsubo, Jpn. J. Appl. Phys. 36 (1997) 1374.
[8] A. S. Grove, Physics and Technology of Semiconductor Devices, John Wiley & Sons, New York (1967).
[9] K.M.Davis and M.Tomozawa, J.Non-Cryst.Solids 201 (1996) 177.
[10] J. W. Osenbach and W. R. Knolle, J. Electrochem. Soc. 139 (1992) 3346.
[11] T. Oku, M. Totsuka and T. Ishikawa, Extended Abstracts (The 50th Spring Meeting, 2003); The Japan Society of Applied Physics and Related Societies, 27a-ZX-9 [in Japanese].